European Polymer Journal 147 (2021) 110319

Contents lists available at ScienceDirect

European Polymer Journal

journal homepage: www.elsevier.com/locate/europolj

Thermal and flame-retardant properties of intrinsic flame-retardant epoxy resin containing biphenyl structures and phosphorus

Xueyan Dai, Peihong Li, Yanlong Sui, Chunling Zhang *

School of Materials Science and Engineering, Jilin University, Changchun 130022, PR China

ARTICLE INFO

Keywords:
Intrinsic flame retardant
Epoxy resin
DOPO
Biphenyl-containing

ABSTRACT

An intrinsic flame-retardant epoxy resin was synthesized by introducing biphenyl structures and phosphorous into epoxy resin. The biphenyl structures could increase the glass transition temperature by more than 10 °C, as well thermal stability as indicated by the elevation in char yield. They could also enhance mechanical properties as reflected by the increments of 86.4% and 176.5% in tensile strength and breaking elongation, respectively, and offset the negative effects of phosphorus-containing structures. The introduction of elemental phosphorus could improve the flame-retardant properties of epoxy resin. The resulting epoxy resin presented a high limiting oxygen index of 32.4% and a V-0 rating in the UL-94 test. Moreover, it exhibited better flame-retardant parameters than pure epoxy resin in the cone calorimeter test. It could be decomposed to generate PO· and PO_2· radicals to quench active free radicals, reduce toxic and smoke gas generation, and form a dense and stable char layer. It could simultaneously achieve gas and condensed phase flame retardancy. The presence of the biphenyl structure and phosphorus element in the epoxy resin system improved the thermal, mechanical, and flame-retardant properties of epoxy resin simultaneously. This work offered a facile method for preparing intrinsic phosphorus-containing flame-retardant epoxy resin without sacrificing thermal and mechanical properties.

1. Introduction

As a high-performance thermosetting resin, epoxy resin has the advantages of excellent chemical stability, dimensional stability, mechanical properties, and simple and diverse curing methods. It has been widely used in electronics, construction, medical and industrial production, and other fields [1–3]. Epoxy resins are mainly composed of carbon, hydrogen, and oxygen, which are essentially highly flammable elements that frequently cause fires during use [4] (see Scheme 1).

The halogen-containing flame-retardant system is the earliest and most widely used flame-retardant system in the world [5,6]. However, it releases a large number of harmful gases and carcinogens during combustion, thus causing non-negligible environmental pollution [7,8]. Given that the use of this system has been strictly restricted at present, developing a halogen-free flame-retardant system is necessary. The halogen-free flame-retardant systems of epoxy resin are mainly divided into inorganic and organic categories. Inorganic flame retardants, including metal hydroxides [9–12], red phosphorus [13–15], silica [16–18], and grapheme [19–21], are added into the matrix via physical dispersion. These retardants have the characteristics of excellent thermal stability, low volatilization, and long-lasting effects. However, they also possess obvious shortcomings, such as large addition amounts, inferior flame-retardant efficiency, poor dispersion and compatibility with the resin matrix, and considerable negative effect on processing and mechanical properties. The organic flame-retardant system is ideal for the flame-retardant modification of epoxy resin; organic phosphorous flame retardants are the most used organic flame-retardant system [22]. The flame-retardant mechanism of organophosphorus flame retardants is to form phosphorus oxygen free radicals in the gas phase to quench the active free radicals generated in combustion and at the same time promote the formation of a dense and stable carbon layer in the condensed phase. It has the advantages of high flame-retardant efficiency, low toxicity, and low smoke generation. Organophosphorus flame retardants can be divided into additive and intrinsic types. Additive flame retardants do not participate in the curing reaction and easily separate from the matrix during long-term storage and use. The latter characteristic reduces resin performance. The melting point of these flame retardants is often higher than the initial curing temperature of epoxy resin, and the compatibility with the system is not good. This will increase the complexity of the epoxy curing process [23]. Intrinsic

* Corresponding author..at: School of Materials Science and Engineering, Jilin University, China, 5988 Renmin St., Changchun, Jilin Prov 130022, China.
E-mail addresses: xydai18@mails.jlu.edu.cn (X. Dai), liph18@mails.jlu.edu.cn (P. Li), suiyl19@mails.jlu.edu.cn (Y. Sui), clzhang@jlu.edu.cn (C. Zhang).

https://doi.org/10.1016/j.eurpolymj.2021.110319
Received 11 January 2021; Received in revised form 18 January 2021; Accepted 22 January 2021
Available online 2 February 2021

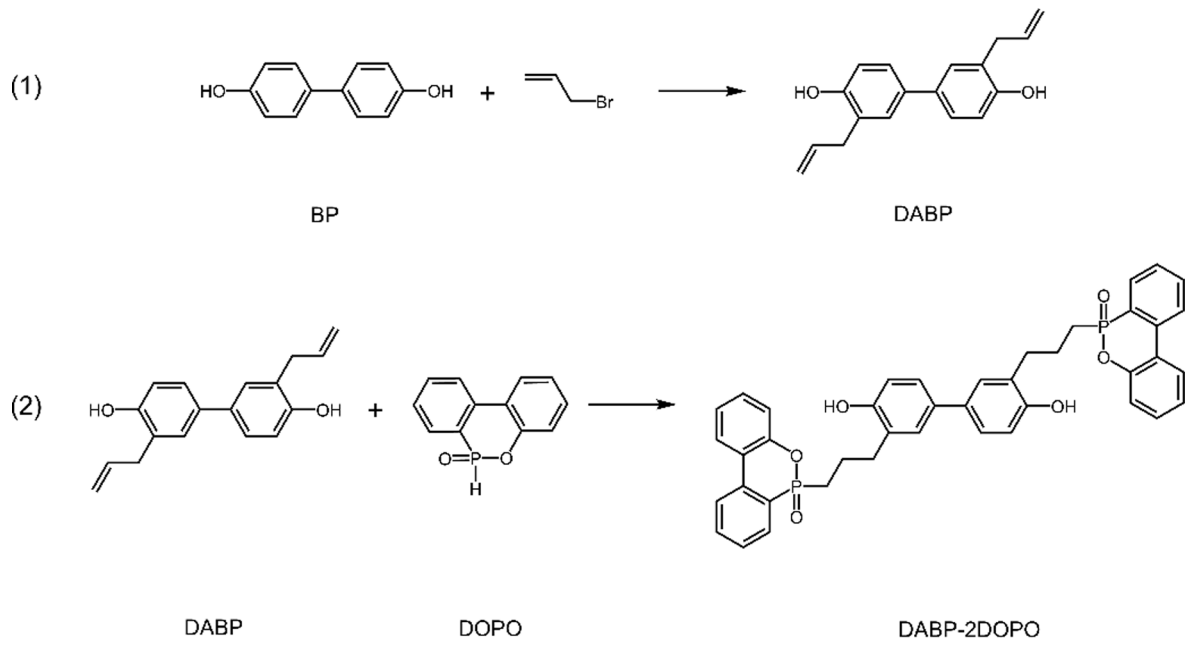

Scheme 1. Synthesis of DABP and DABP–2DOPO.

flame retardants are connected to the matrix resin through chemical bonds, participate in curing, and become a component of the cured system structure [24–26]. Although they ensure flame-retardant performance, they have a negligible effect on the curing process, thermal properties, mechanical properties, and other properties.

9,10-Dihydro-9-oxa-10-phosphaphenanthrene-10-oxide (DOPO) is a commonly used organic phosphorous flame retardant [27,28]. The P–H bond in the DOPO structure is a highly reactive chemical bond that can be added to olefins and epoxy groups to synthesize a series of DOPO derivatives [28]. Epoxy resins containing DOPO have excellent flame-retardant capabilities. However, the lower bond energy of P–C and P–O than that of C–C leads to a reduction in the thermal stability of polymers. In addition, DOPO hinders the cross-linking reaction and increases the brittleness of the resin, thus greatly reducing mechanical properties, because of its strong steric hindrance and rigidity [29–32]. Therefore, improving flame-retardant properties without sacrificing other properties has become the key to the research on DOPO-containing flame-retardant epoxy resins.

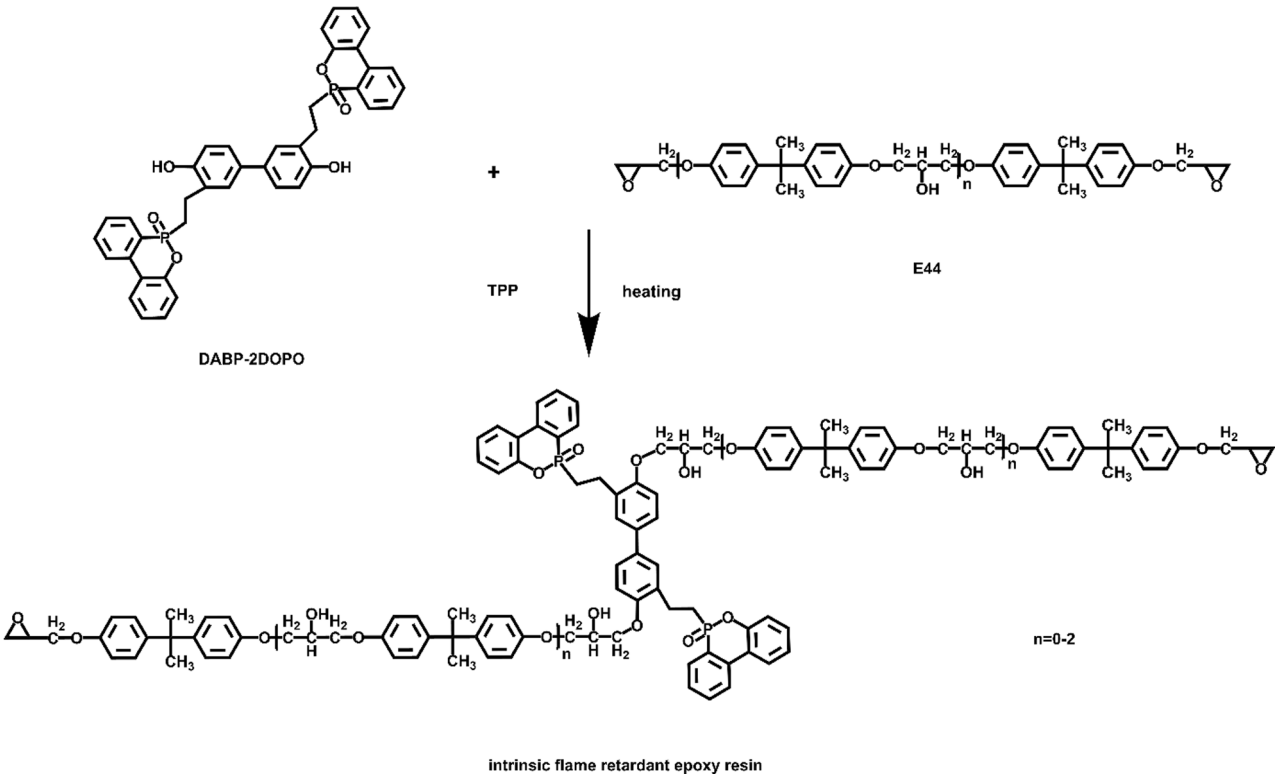

Scheme 2. Preparation of intrinsic flame-retardant epoxy resin.

Table 1
Sample formulations and epoxy value of the intrinsic flame-retardant epoxy resin.

Sample	E44 (g)	DABP-2DOPO (g)	E[a] (mol/100 g)	DDM (g)	P content (wt.%)	Curing procedures[b]		
						T_i[c] (°C)	T_p[d] (°C)	T_f[e] (°C)
EP	100	0	0.475	23.5	0	80.0	130.0	180.0
EP/1%DABP-2DOPO	100	1	0.467	23.3	0.07	78.8	127.6	186.8
EP/5%DABP-2DOPO	100	5	0.456	23.7	0.34	72.6	130.8	194.9
EP/10%DABP-2DOPO	100	10	0.423	23.0	0.67	81.4	129.7	196.9

[a] : The epoxy value of the intrinsic flame-retardant epoxy resin.
[b] : The curing procedure of EP was selected in accordance with the curing temperature of commercial epoxy resin products while the curing procedures of the EP/DABP–2DOPO system were obtained via curing kinetics studies.
[c] : Initial curing temperature.
[d] : Peak curing temperature.
[e] : Final curing temperature.

In this work, we first synthesized a bisphenol with allyl groups (DABP) via Williamson ether synthesis and Claisen rearrangement reaction. Then, a biphenyl/phosphorous-containing reactive flame retardant (DABP–2DOPO) was synthesized through the addition reaction of DABP and DOPO and cured with E44/4,4-diaminodiphenyl methane (DDM) to prepare an intrinsic flame-retardant epoxy resin. This intrinsic flame-retardant epoxy resin contained biphenyl structures and low amounts of phosphorus. The introduction of phosphorus elements could improve the flame-retardant properties of epoxy resins, and the biphenyl structure could offset the problems, such as decreased thermal stability, caused by phosphorus-containing structures and improve the mechanical properties of epoxy resins.

2. Experimental

2.1. Materials

Allyl bromide and 4,4′-dihydroxybiphenyl (BP) were purchased from Macklin Biochemical Co., Ltd. (Shanghai, China). Anhydrous potassium carbonate (K_2CO_3), triphenylphosphine (TPP), DOPO, and DDM were provided by Aladdin Industrial Corporation (Shanghai, China). Ethanol and n-heptane were obtained from Beijing Chemical Works (Beijing, China). Epoxy resin (E44) was supplied by Wuxi Dic Epoxy Co., Ltd, with an epoxy value of 0.44 mol/100 g.

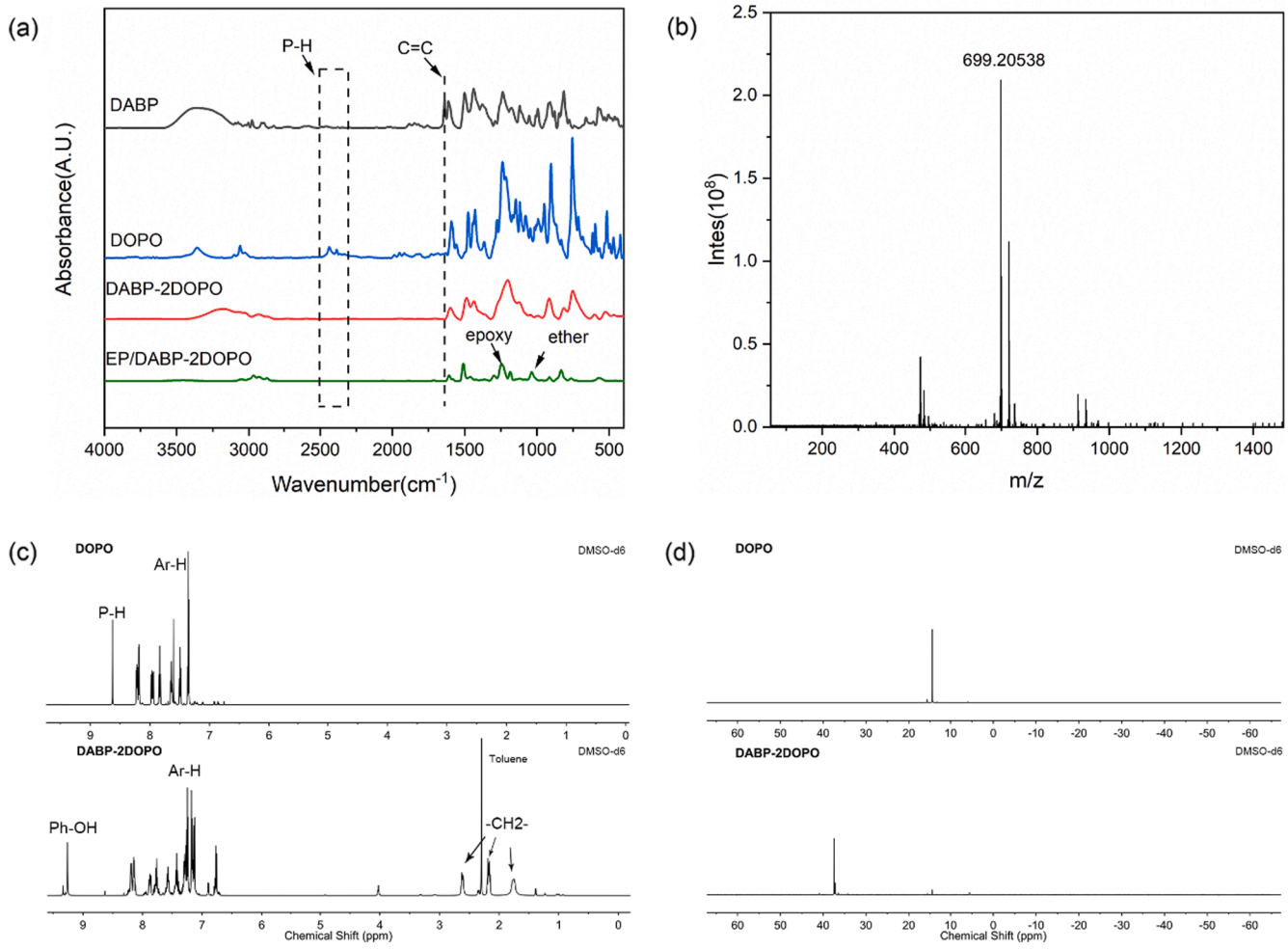

Fig. 1. Characterization of DABP–2DOPO: (a) FT–IR spectra, (b) HRMS, (c) ^{1}H NMR, and (d) ^{31}P NMR.

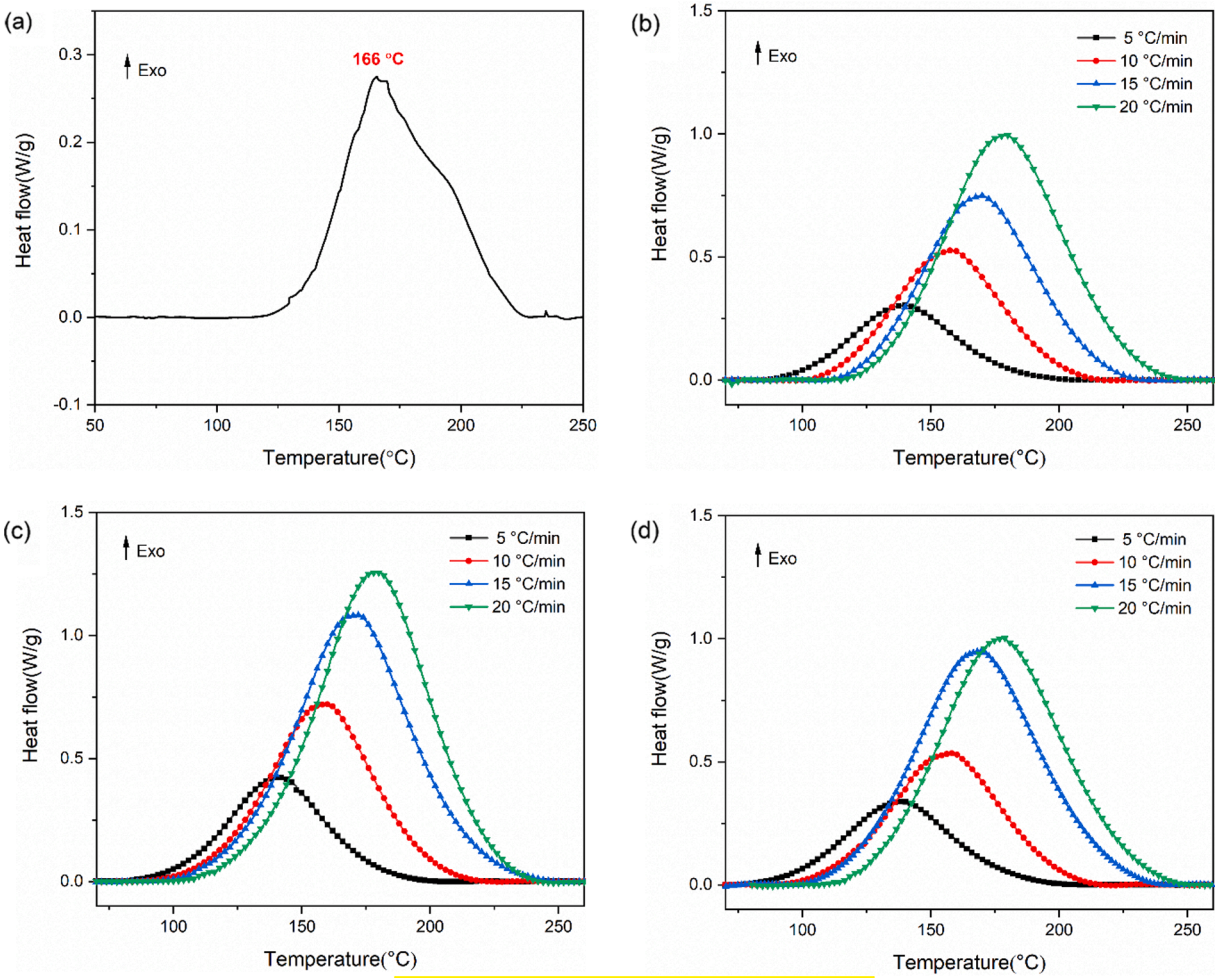

Fig. 2. Characterization of the intrinsic flame-retardant epoxy resin by DSC: (a) the possibility of reaction between DABP–2DOPO and E44; (b), (c), and (d) curing kinetics studies on EP/1%DABP–2DOPO, EP/5%DABP–2DOPO, and EP/10%DABP–2DOPO.

2.2. Sample preparation

2.2.1. Preparation of DABP–2DOPO

BP (18.62 g, 0.1 mol), K_2CO_3 (27.64 g, 0.2 mol), and ethanol were placed in a three-necked flask and mixed at 75 °C for 1 h. Then, allyl bromide (26.62 g, 0.22 mol) was slowly added and reacted for 8 h. A solid was obtained by washing and drying and then heated to 210 °C for 2 h under a nitrogen atmosphere for the Claisen rearrangement reaction. After the reaction was completed, the solution was recrystallized in n-heptane and dried to obtain DABP.

^{1}H NMR (600 MHz, chloroform-d) δ (ppm): 7.34 (d, 2H), 6.89 (d, 1H), 6.09 (ddt, 1H), 5.30–5.16 (m, 2H), 3.50 (dd, 2H).

DOPO (21.6 g, 0.1 mol) was added into a three-necked flask at 130 °C with stirring until completely melted. Then, DABP (13.2 g, 0.05 mol) was added in batches into the reaction system. Subsequently, the system temperature was increased to 160 °C, and stirring was continued for 6 h. DABP–2DOPO was obtained after cooling to room temperature.

^{1}H NMR (600 MHz, DMSO-d_6): δ 9.26 (s, 1H), 8.19 (dd, 1H), 8.16–8.12 (m, 1H), 7.87 (dd, 1H), 7.76 (t, 1H), 7.57 (td, 1H), 7.43 (t, 1H), 7.33–7.27 (m, 1H), 7.25 (s, 1H), 7.18 (s, 1H), 7.13 (s, 1H), 6.77 (t, 1H), 2.66–2.57 (m, 2H), 2.22–2.13 (m, 2H), 1.77 (q, 2H).

^{31}P NMR (243 MHz, DMSO-d_6): a single peak at δ 37.45 (d, $J = 6.8$ Hz).

HRMS:[M + 1$^+$], found 699.20538.

2.2.2. Preparation of intrinsic flame-retardant epoxy resin

DABP-2DOPO and E44 were reacted at 165 °C under the catalysis of TPP to obtain the intrinsic flame-retardant epoxy resin as illustrated in Scheme 2. The additive amounts of DABP-2DOPO were 0%, 1%, 5%, and 10%, respectively (based on the quality of E44).

2.2.3. Preparation of cured epoxy resin

The intrinsic flame-retardant epoxy resin and DDM were mixed with stirring at 80 °C, and the blend was placed into the oven for curing. The cured epoxy resins were named as EP, EP/1%DABP–2DOPO, EP/5% DABP–2DOPO, and EP/10%DABP–2DOPO. Their formulations are listed in Table 1. The curing procedures were obtained via curing kinetics studies.

2.3. Characterization

FT–IR spectra were recorded over the range of 4,000–400 cm^{-1} at a resolution of 4 cm^{-1} on a Nicolet Nexus 670 spectrometer. ^{1}H NMR and ^{31}P NMR spectra were recorded on a Bruker Avance-600 spectrometer in chloroform-d and DMSO-d_6. High-resolution mass spectrometry analysis was performed on a Bruker solanX 70 FT-MS. Thermogravimetric analysis (TGA, Netzsch TG 209F3, Netzsch) was conducted under nitrogen at a heating rate of 10 °C/min to investigate thermal stability. DSC was performed by using a TA Q20 differential scanning calorimeter to study glass transition behavior and curing kinetics. A dynamic thermodynamic analyzer (DMA, DMA + 450, 01-db Metravib) was used to study thermomechanical properties at a heating rate of 5 °C/min at 1 Hz. The tensile test was carried out by using an Instron-1121 electronic universal testing machine in accordance with GBT 2567–2008. Cone

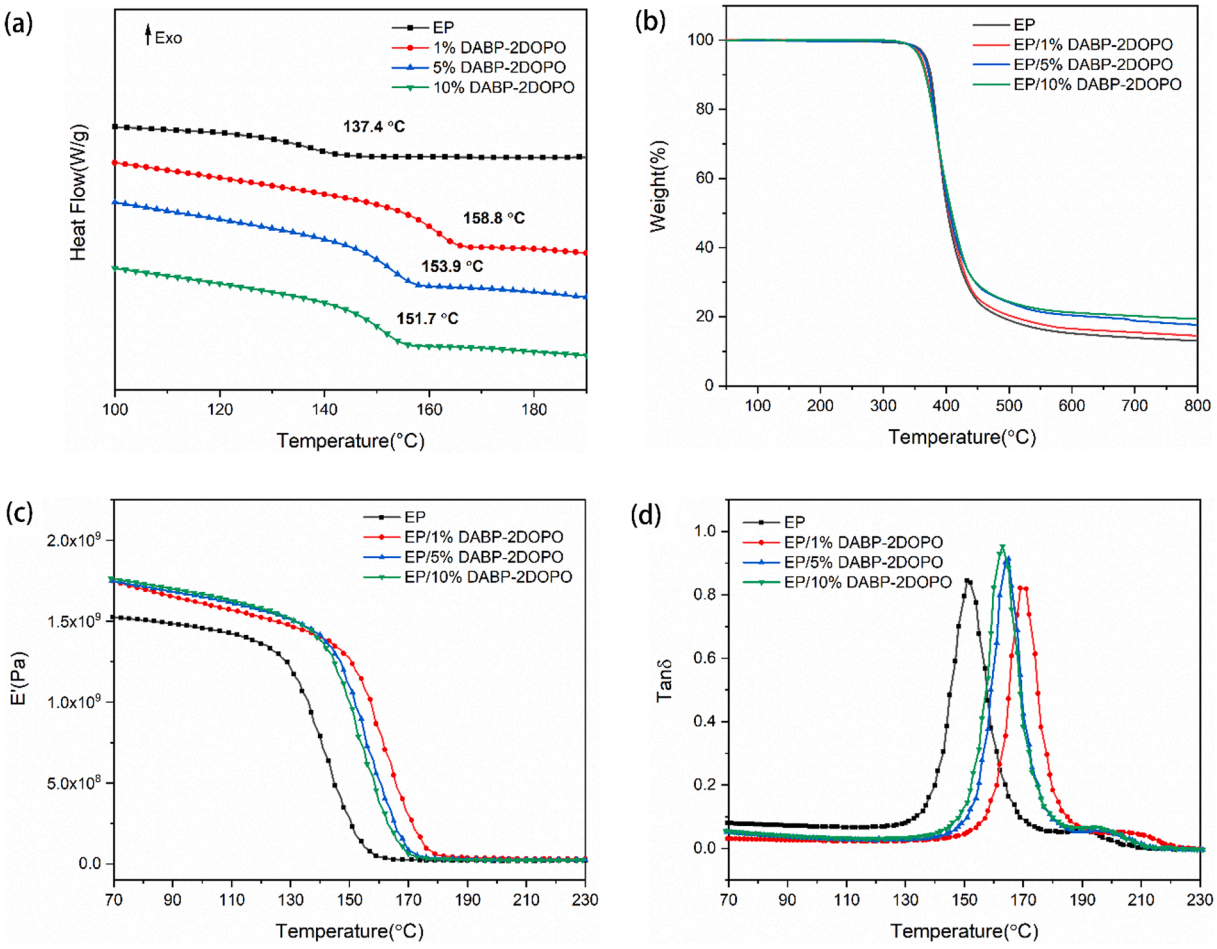

Fig. 3. Thermal analysis of cured epoxy resin (EP, EP/1%DABP–2DOPO, EP/5%DABP–2DOPO, and EP/10%DABP–2DOPO): (a) DSC curves, (b) TG curves under N_2, (c) and (d) DMA curves of the storage modulus and loss tangent.

calorimetric measurements were taken on a Fire Testing Technology FTT0007 apparatus in accordance with ISO 5660 (sample size: 100 mm × 100 mm × 3 mm). Scanning electron microscopy (SEM, XL-30, FEI Company) with an acceleration voltage of 10 kV was utilized to observe char morphologies. The limiting oxygen index (LOI) was tested by using a LOI meter (FESTEC JF-3, Korea) with ASTMD-2863–97. The vertical burning test was conducted with a vertical burning tester (Motis Fire Technology UL94-X, China) with ASTMD 3801. The thermogravimetry–infrared test (TG–IR) was performed by using a Nicolet 6700 instrument, and Raman spectra were acquired with Renishaw Raman spectrometer. XPS analysis was carried out by using Thermal ECSALAB 250 with an Al anode.

3. Results and discussion

3.1. Characterization of DABP–2DOPO

The reactive flame-retardant DABP–2DOPO was synthesized through the addition of DOPO to DABP. The FT–IR spectra of the material are presented in Fig. 1(a). The characteristic bands at 3339, 2972, and 1638 cm^{-1} in the spectrum of DABP corresponded to the stretching vibrations of Ph—OH, —CH_2— and C═C. The bands at 2441, 1592, 1276, and 1078 cm^{-1} in the spectrum of DOPO belonged to the stretching vibrations of P—H, P—Ph, P═O, and P—O—Ph. As the reaction proceeded, the characteristic bands at 2441 cm^{-1} for the P—H band in DOPO and 1638 cm^{-1} for the allyl group in DABP disappeared while the broad characteristic band of phenolic hydroxyl shifted from 3339 cm^{-1} to 3190 cm^{-1}. The ^{1}H NMR and ^{31}P NMR spectra of DABP–2DOPO are shown in Fig. 1(c) and (d). The peaks at 1.77, 2.17, and 2.61 ppm were assigned to —CH_2—, the peaks at 6.77–8.19 ppm corresponded to Ar—H, and the peak at 9.26 ppm was attributed to Ph—OH. The peak of P–H at 8.63 ppm and the peaks of the allyl group at 5.0 and 6.0 ppm disappear in DABP-2DOPO. The peak in ^{31}P NMR was shifted from 14.48 ppm to 37.45 ppm as shown in Fig. 1(d). The structures of DABP–2DOPO were further proven by the HRMS spectra in Fig. 1(b). The results of FT–IR, NMR, and HRMS confirmed that DABP–2DOPO was successfully synthesized.

3.2. Characterization of the intrinsic flame-retardant epoxy resin

DSC was used to explore the possibility of the reaction of DABP–2DOPO with E44. Only one exothermic peak was observed at 166 °C in Fig. 2(a). This peak represented the ring-opening reaction of the phenolic hydroxyl and epoxy groups [33]. The FT–IR spectra of the intrinsic flame-retardant epoxy resin are presented in Fig. 1(a). The characteristic bands at 1243 and 1039 cm^{-1} corresponded to the epoxy and ether groups. The results of DSC and FT–IR could prove that DABP–2DOPO was a kind of reactive flame-retardant that could be used to prepare intrinsic flame-retardant epoxy resins. The intrinsic flame-retardant epoxy resins were obtained by adding different proportions of DABP–2DOPO for reaction with E44. The epoxy value of the intrinsic flame-retardant epoxy resin was measured via the hydrochloric acid–acetone method, and the results are listed in Table 1. As the content of DABP–2DOPO was increased, the epoxy value decreased. A non-isothermal curing kinetics study was carried out by using DSC to determine curing parameters. Fig. 2(b), (c), and (d) show the DSC

Table 2
Thermal parameters of cured epoxy resin.

Sample	$T_{g,\ DSC}$ (°C)	$T_{g,\ DMA}$ (°C)	Modulus at 50 °C ($\times 10^9$ Pa)	ν_e ($\times 10^3$ mol/m^3)	$T_{5\ wt.\%}$ (°C)	T_{max} (°C)	char yield (wt.%)
EP	137.4	151.0	1.55	2.39	367.3	384.7	12.6
EP/1%DABP-2DOPO	158.8	170.0	1.86	3.59	364.3	389.3	14.5
EP/5%DABP-2DOPO	153.9	164.9	1.79	2.85	360.2	385.5	17.7
EP/10%DABP-2DOPO	151.7	163.4	1.80	2.55	357.7	382.7	19.4

thermograms obtained at the different heating rates of 5, 10, 15, and 20 °C/min, and the data from curing kinetics studies are listed in Table 1. The same curing temperature was selected for curing. The activation energy of the curing process could be calculated by using the Kissinger equation [34] and the Ozawa equation [35].

Kissinger equation:

$$\frac{d(\ln(\beta/T_p^2))}{d(1/T_p)} = -\frac{E_a}{R} \quad (1)$$

Ozawa equation:

$$\frac{d(\ln\beta)}{d(1/T_p)} = -1.052\frac{E_a}{R} \quad (2)$$

where β is the heating rate, T_p is the peak curing temperature, E_a is the apparent activation energy, R is the gas constant, and n is the reaction order. According to the Kissinger method, the activation energy values of EP/1%DABP–2DOPO, EP/5%DABP–2DOPO, and EP/10% DABP–2DOPO were 45.98, 49.05, and 45.48 kJ/mol, respectively. The activation energy values calculated through the Ozawa method were 50.50, 53.42, and 50.03 kJ/mol.

3.3. Thermal analysis

The thermal performance of the cured epoxy resin was determined via DSC, TGA, and DMA as shown in Fig. 3, and the data are summarized in Table 2. The glass transition temperature (T_g) is one of the characteristic temperatures of polymers. It directly affects the use and process performances of materials. DSC and DMA were used to determine the T_g of cured epoxy resins. The DSC method is based on the change in the heat capacity of the polymer during the transition from the glassy state into the high-elastic state. The T_g of EP was observed at 137.4 °C as depicted in Fig. 3(a). When DABP–2DOPO was added, the T_g of epoxy resins exceeded 150 °C. As the content of DABP–2DOPO was increased, the T_g of epoxy resins inversely decreased. The DMA method is a technique that is based on measuring the mechanical properties and viscoelastic properties of a sample under periodic vibration stress with temperature or frequency. The DMA method is more sensitive than the DSC method. The DMA method also provides the cross-link density (ν_e) of epoxy resins, which can be calculated by using the following equation:

$$\nu_e = E_r^{'}/3RT_r \quad (3)$$

where $T_r = T_{g,\ DMA} + 30$ °C, $E_r^{'}$ is the storage modulus at T_r, R is the gas constant, and ν_e is the cross-link density. The data measured by DMA had the same trend as that measured by DSC. The T_g and ν_e of epoxy resins greatly increased after the addition of DABP–2DOPO and showed a downward trend as the content of DABP–2DOPO was increased. T_g is mainly determined by molecular structure and cross-linking density. The storage moduli of the samples were 1.55, 1.86, 1.79, and 1.80 $\times 10^9$ Pa, respectively. The high rigidity of biphenyl and DOPO increased the storage modulus with the addition of DABP–2DOPO. In terms of molecular structure, DABP–2DOPO contained a rigid biphenyl backbone and bulky side group (DOPO). It could increase the rigidity of the molecular chain, create a motion barrier, hinder the movement of the molecular chain, and increase T_g. On the other hand, the steric hindrance effect of the bulky side groups loosened the molecular chain arrangement [36]. Hence, molecular distance increased, free volume increased, and cross-link density decreased. These effects led to a reduction in T_g.

The thermal stability of EP, EP/1%DABP–2DOPO, EP/5% DABP–2DOPO, and EP/10%DABP–2DOPO was characterized via TGA as shown in Fig. 3(b). All samples had only one decomposition stage within the test range. This stage was the rupture of the main chain in the cross-linked network. Given that the bond stability of O═P—O and P—C was lower than that of C—C [25,26], the value of 5% degradation temperature ($T_{5\ wt.\%}$) dropped slightly when DABP–2DOPO was added to the epoxy resin. $T_{5\ wt.\%}$ gradually decreased with the increase in addition amount. The temperature of maximum degradation (T_{max}) did not show a downward trend such as that shown by $T_{5\ wt.\%}$. The EP/DABP–2DOPO system contained rigid biphenyl structures both in the DOPO group and main chain of the polymer. Also, the cross-link density of EP/DABP–2DOPO was higher cross-link density than EP. It could offset the negative effect of phosphorus-containing structure on the thermal stability and maintain the T_{max} above 380 °C. Also, due to the presence of the aromatic biphenyl structure, the char yield of the EP/DABP–2DOPO system was significantly higher than that of EP, and the char yield of EP/10%DABP–2DOPO reached the maximum value of 19.4%. The increase in char yield showed that DABP–2DOPO had a good catalytic capability to form char and could improve the stability of epoxy resin at high temperature [37]. The combined results of DSC, DMA, and TGA could prove that the addition of DABP–2DOPO could improve the thermal properties of epoxy resin, thereby contributing to the improvement in flame retardancy.

3.4. Flame-retardant properties of epoxy resin

First, UL-94 and LOI tests were performed on the epoxy resin samples. The resulting data are listed in Table 3. The LOI value of EP was 26.9% and that of EP/10%DABP–2DOPO was 32.4%. The value of LOI was directly related to the char yield of the polymer. The polymer with a high char yield had a high LOI value likely because the formation of char could reduce volatile generation and affect thermal degradation behavior. After the surface of the epoxy resin was wrapped by the char layer, the interior was isolated from the flame. This effect made further thermal degradation difficult. Furthermore, the main chain contained a large amount of biphenyl structures that increased aryl group content and promoted char aromatization. The pure epoxy resin of E-44 had no rating in the UL-94 test [38]. As could be seen from Fig. 4, the EP began to burn violently until the entire sample was completely deformed. EP/

Table 3
UL-94, LOI, and cone calorimetry data of EP and EP/10%DABP–2DOPO.

Sample	UL-94	LOI (%)	TTI (s)	PHRR (kW/m^2)	THR (MJ/m^2)	Residual mass (%)	Av-EHC (MJ/kg)	TSR (m^2/m^2)	TSP (m^2)
EP	No rating	26.9 ± 0.4	80	1198.8	107.5	10.8	30.6	3605.2	32.2
EP/10% DABP–2DOPO	V-0	32.4 ± 0.3	73	877.6	90.9	16.4	27.6	2891.5	25.8

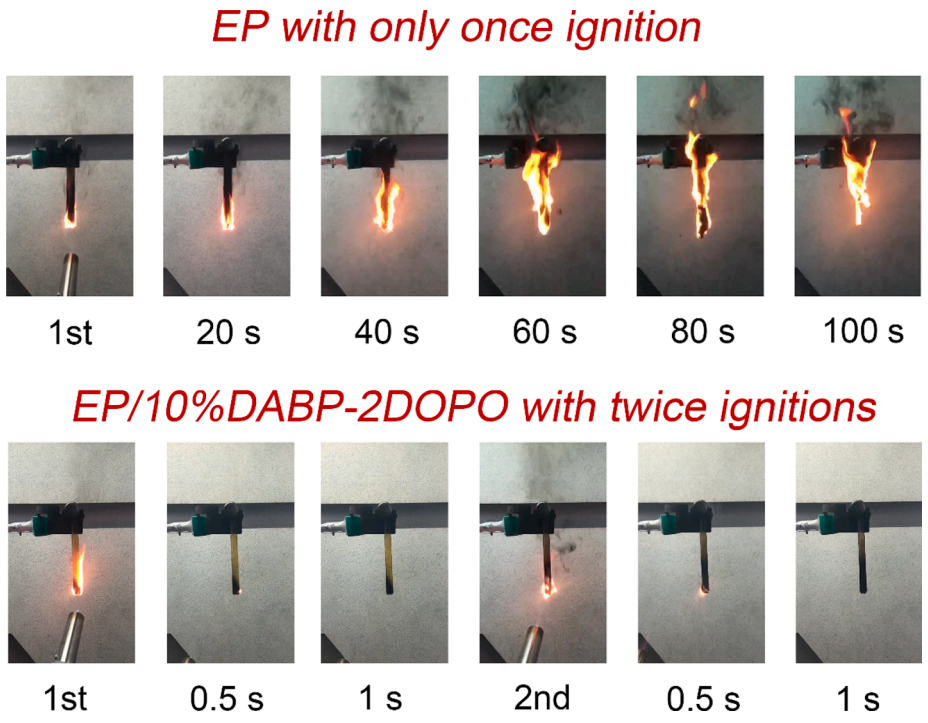

Fig. 4. Digital photographs of UL-94.

10%DABP–2DOPO was extinguished quickly within 10 s after being ignited twice. It presented a V-0 rating. UL-94 and LOI demonstrated that the self-extinguishing property of EP/10%DABP–2DOPO was stronger than that of EP.

As shown in Figs. 5 and 6, TG–IR was used to analyze the volatile gas products that were generated during combustion. The characteristic peaks of H_2O/phenol, hydrocarbons, carbon monoxide, carbon dioxide, carbonyl compounds, aromatic compounds, and ether compounds could be observed in EP and EP/10%DABP–2DOPO during the thermal decomposition process. As shown in Fig. 5(b), the characteristic peak of P-containing compounds appeared at 1058 cm^{-1}. Simultaneously, the characteristic peak of P-containing compounds was also observed at T_{max} as illustrated in Fig. 5(c). The P-containing compounds mainly included PO· and PO_2· radicals that were generated by the decomposition of the DOPO structure, which could eliminate the combustible H· and OH· in the combustion system. Fig. 6(a–f) show the intensity changes in volatile gas. Compared with that in EP, the intensity of total volatile products in EP/10%DABP–2DOPO had decreased. Moreover, the intensities of CO, CO_2, hydrocarbons, carbonyl compounds, and aromatic compounds in this material were all lower than those in EP. This result indicated that the addition of DABP–2DOPO could reduce smoke production and toxic gas production.

The cone calorimeter test is a method that is widely used to determine flame retardancy properties and multiple parameters for evaluating flammability [39]. Fig. 7 and Table 3 show the results of the cone calorimeter test. Time to ignition (TTI) can reflect the influence of a flame retardant on ignitability [40]. The TTI value of EP/10% DABP–2DOPO decreased from 80 s to 73 s because EP/10% DABP–2DOPO had a lower initial temperature and released small molecules earlier than EP. Heat release rate (HRR) and peak heat release rate (PHRR) can be applied to predict fire hazards and are the most important parameters in the cone calorimeter test. The PHRR of EP was 1198.8 kW/m^2 and that of EP/10%DABP–2DOPO was 877.6 kW/m^2. Meanwhile, compared with those of EP, the total heat release (THR) and average effective heat of combustion (av-EHC) of EP/10%DABP–2DOPO had decreased by 15.4% and 9.8%, respectively. The mass of the char residuals of EP/10%DABP–2DOPO was 16.4%, whereas that of EP was only 10.8%. The trend observed in this test was the same as that shown in TGA. The reduction in PHRR, THR, and av-EHC might be attributed to the generation of a stable and dense char during combustion that would form a physical barrier to limit heat exchange. This phenomenon also indicated that the heat released by the fire source decreased. Consequently, the spread of flames decreased because the reduction in heat feedback from combustion to the surface of the material would lower the pyrolysis rate of the material and the generation of volatile combustibles. The total smoke release (TSR) and total smoke production (TSP) of EP/10%DABP–2DOPO decreased by 19.8% and 19.9%, respectively. The decrement in smoke performance parameters might be due to the increment in char formation capacity during combustion, and the dense and stable char layer inhibited the generation and release of smoke. The decreases in TSR and TSP were due to the thermal stability of the polymer and the increased char yield, which promoted char layer formation in the condensed phase and reduced volatile product generation.

Furthermore, the char residuals were characterized based on Raman spectra, XPS, and SEM. As illustrated in Fig. 8(a) and (b), a large number of through-holes and cracks could be observed in the char residuals of EP. These structures could provide channels for the transport of combustible volatile gas and promote combustion. The char residuals of EP/10%DABP–2DOPO are presented in Fig. 8(c) and (d) and show a compact and smooth morphology with few cracks and no holes. Fig. 8(e) depicts that the char layer had a large amount of phosphorus. Except for the formation of phosphorus oxygen free radicals, most of the phosphorus elements remained in the condensed phase. This situation catalyzed the production of char residuals and promoted the formation of a dense and stable char layer, which could be used as a physical barrier to block the volatilization of combustible gases and protect the internal structure. The digital photos in Fig. 9 show that the char layer had formed a complete shell. Fig. 10(a) and (b) provide the Raman spectra of the char residuals. D band represented the lattice defect while the G band represented the in-plane stretching vibration of sp^2 hybridization of C atoms. The intensity ratio of the D band and G band (I_D/I_G) decreased, the number of lattice defects decreased, the degree of sp^2 hybridization increased, and the degree of char graphitization increased. When DABP–2DOPO was added, the value of I_D/I_G decreased from 2.64

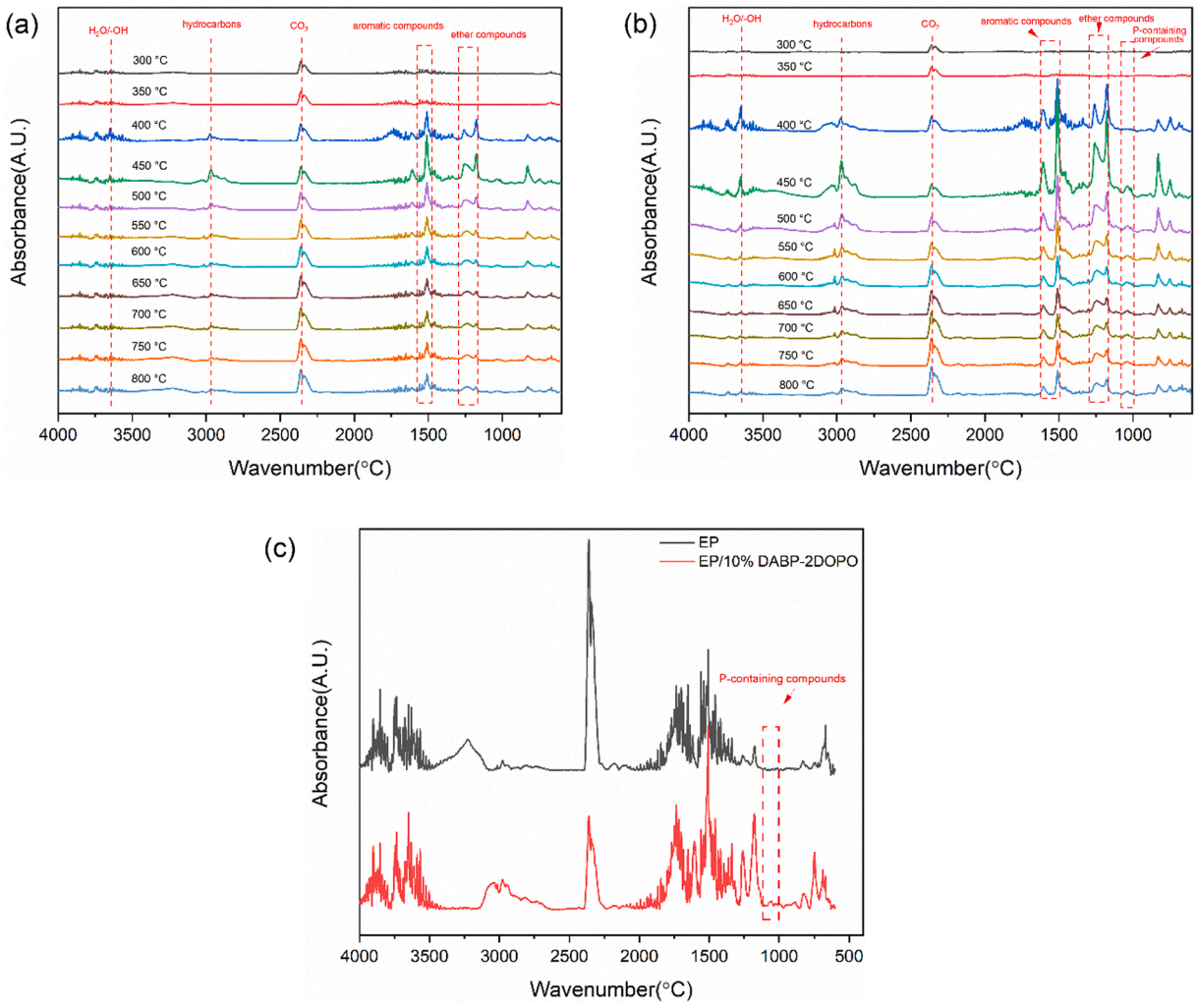

Fig. 5. FT–IR spectra of volatile products: (a) EP, (b) EP/10% DABP–2DOPO, and (c) EP and EP/10% DABP–2DOPO at T_{max}.

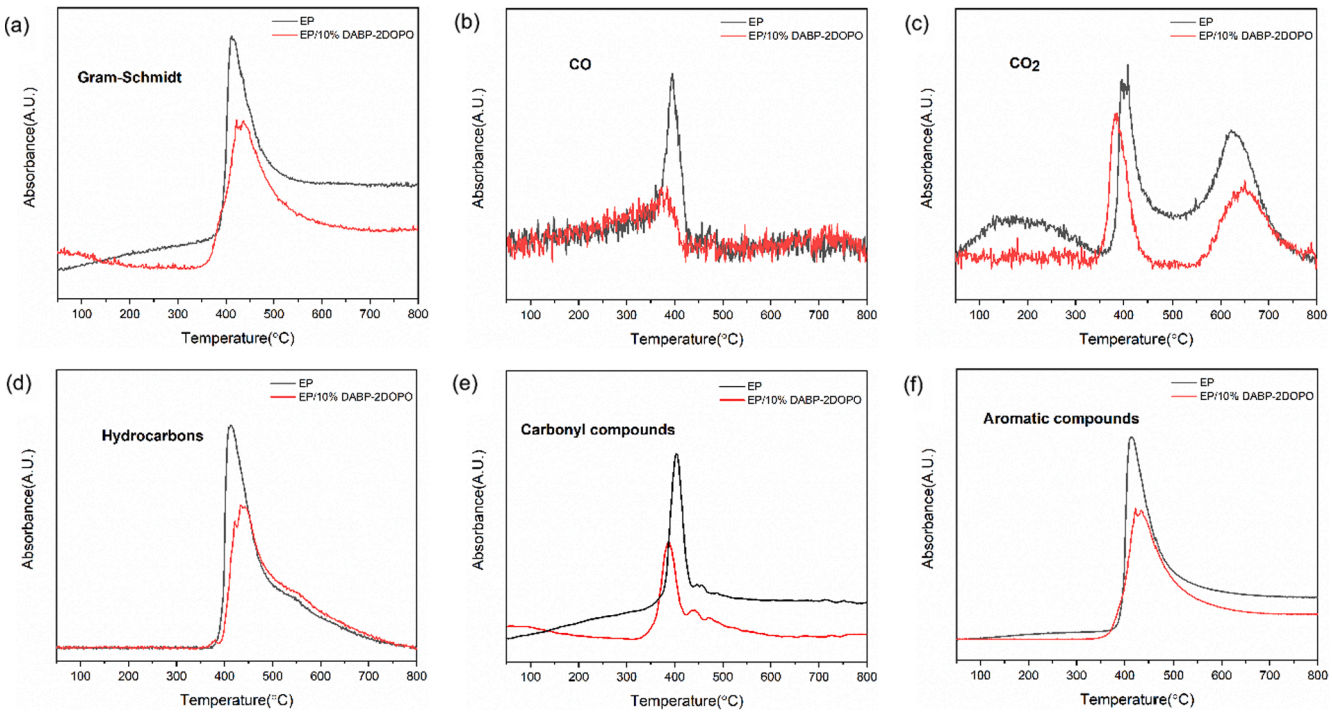

Fig. 6. The absorbance peaks of volatile products of EP and EP/10% DABP–2DOPO.

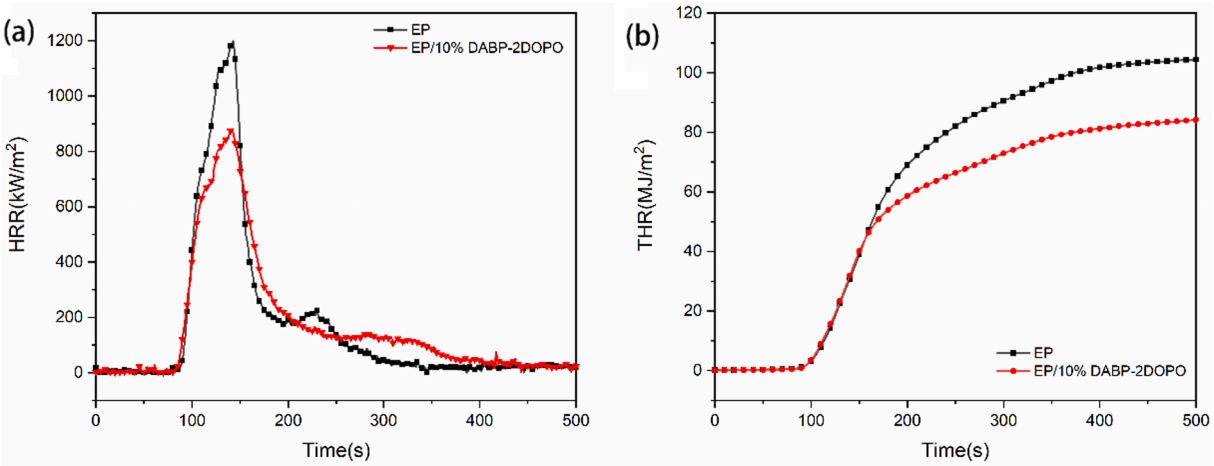

Fig. 7. Cone calorimetry test parameters of EP and EP/10%DABP–2DOPO: (a) HRR curves, (b) THR curves.

to 2.41, indicating that the incorporation of DABP–2DOPO could enhance graphitization. The C1s and P2p spectra of char residuals were acquired via XPS and are given in Fig. 10(c–e). The C—C bond ratio of EP was 60.0%, whereas that of EP/10%DABP–2DOPO was 65.3%. Similar to the results of the Raman spectrum, the increase in this ratio proved that the graphitization degree of char residuals had increased. Moreover, the char residuals of EP/10%DABP–2DOPO showed the characteristics of P—C (133.4 eV), P—O (134.3 eV), and P═O (135.1 eV) as illustrated in Fig. 10(e) [41]. These characteristics indicated that EP/10DABP–2DOPO could generate a phosphorus-rich char layer after combustion. EP/10%DABP–2DOPO contained a large amount of biphenyl structures. Rigid aromatic rings could improve the aromatization of the char layer, thereby improving the regularity of the char layer and graphitization and generating a dense and stable phosphorus-rich char layer.

3.5. Analysis of mechanical properties

The tensile properties of the EP and the EP/DABP–2DOPO system are shown in Fig. 10. The stress–strain curves in Fig. 11(a) show that EP and the EP/DABP–2DOPO system exhibited typical brittle fracture behavior. As illustrated in Fig. 11(b), the tensile strength and breaking elongation of EP were 32.3 MPa and 3.4%, respectively. When the amount of DABP–2DOPO added was 1%, tensile strength and breaking elongation

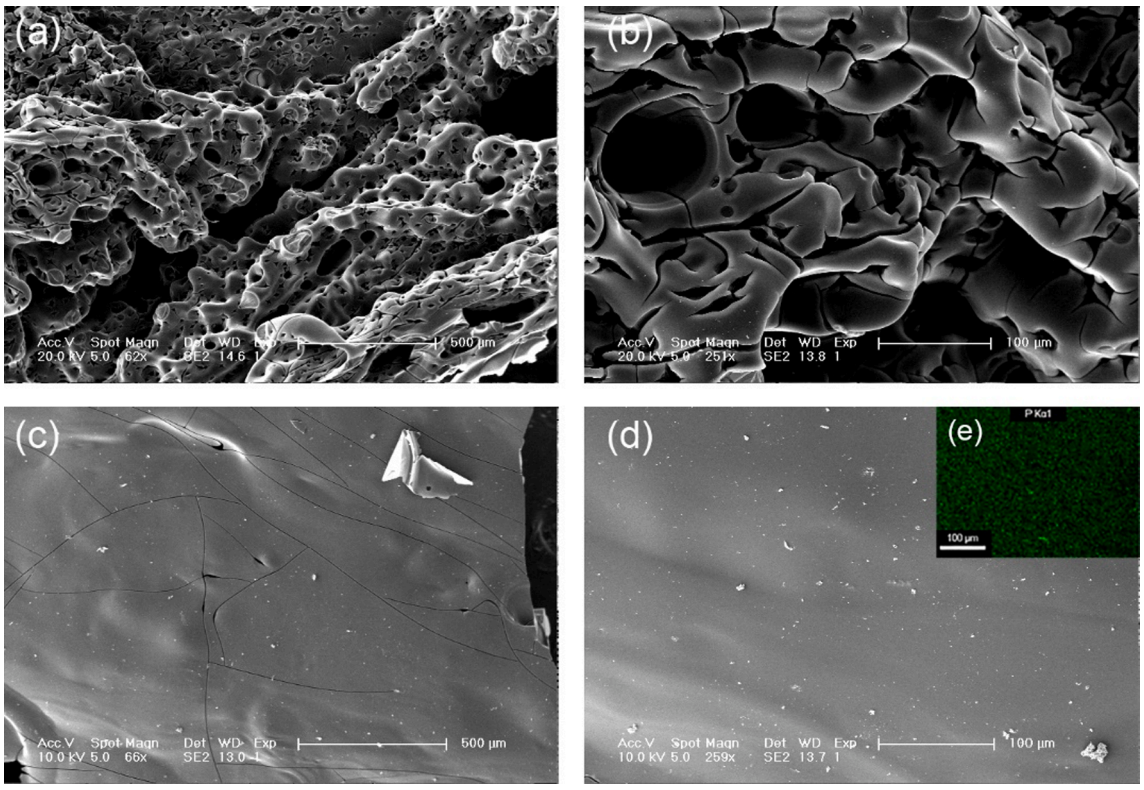

Fig. 8. Char residuals structures by SEM: (a) and (b) EP, (c) and (b) EP/10%DABP–2DOPO, and (e) EDS results of EP/10%DABP–2DOPO: P elemental mapping distribution.

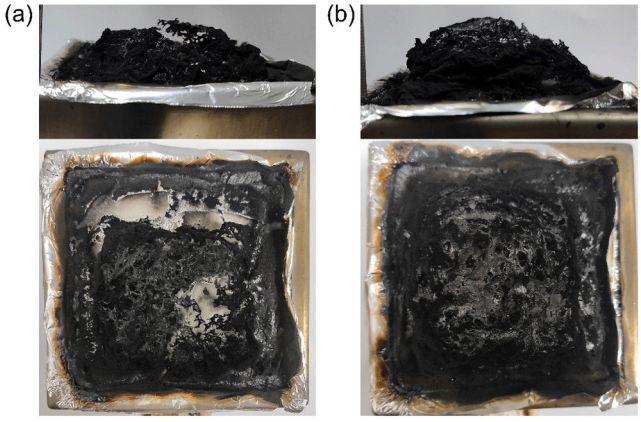

Fig. 9. Digital photo of the char residuals: (a) EP, (b) EP/10%DABP–2DOPO.

increased by only 14.2% and 5.0%, respectively, because the small additional amount had a weak impact on tensile properties. Tensile strength and breaking elongation significantly improved with the increase in additive amount. Tensile strength increased by 51.7% and 86.4%, and the breaking elongation at break increased by 91.2% and 176.5%. EP/10%DABP–2DOPO showed the best tensile properties. Generally, DOPO and its derivatives are used as additives in DOPO-containing epoxy resin systems. The mechanical properties of the epoxy resin were greatly reduced given the poor compatibility of DOPO with the matrix and large steric hindrance. Introducing DOPO into the epoxy resin structure to prepare intrinsic DOPO epoxy resin could solve the compatibility problem. The biphenyl structure and the DOPO group showed great rigidity, which enhanced the rigidity of epoxy resin and subsequently led to an increase in the tensile strength of epoxy resin. Moreover, the DOPO group was located in the side group, and the space group $(CH_2)_3$ was present between the main chain and the DOPO group. The space group had great flexibility, which could weaken the steric hindrance of DOPO and enhance the mobility and flexibility of the side chain. Thus, the breaking elongation of EP/DABP–2DOPO was higher than that of EP. With the increase in DABP–2DOPO, the increase in side chains and the decrease in cross-linking density would simultaneously lead to an increase in breaking elongation.

4. Conclusions

As proven via FT–IR, NMR, and HRMS analyses, a biphenyl/phosphorous-containing intrinsic flame-retardant epoxy resin was successfully prepared by introducing DABP–2DOPO. The curing program and activation energy of the EP/DABP–2DOPO system were determined via nonisothermal curing kinetics. The glass transition temperature and thermal stability of the EP/DABP–2DOPO system had significantly improved over those of EP after the addition of DABP–2DOPO. EP/10% DABP–2DOPO exhibited excellent flame retardancy, and its flame-retardant mechanism was mainly the condensation mechanism and the gas phase mechanism. During combustion, the intrinsic flame-retardant epoxy resin generated PO· and PO_2· free radicals which could quench the highly active H· and HO· free radicals produced by pyrolysis and interrupt the free radical reaction of combustion. The biphenyl structure in the main chain of epoxy resin could improve the condensed phase effect of DOPO. The intrinsic flame-retardant epoxy

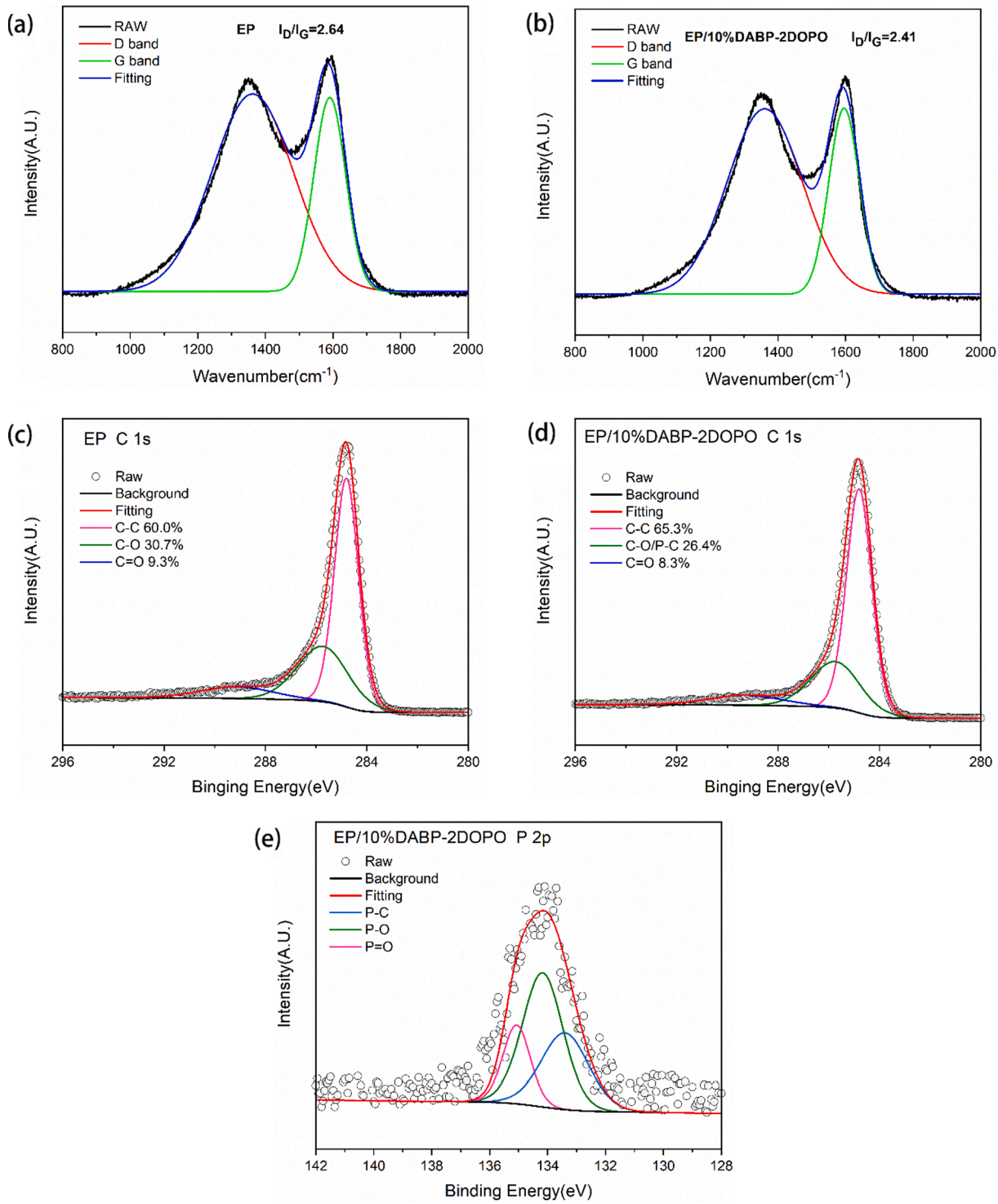

Fig. 10. (a) and (b) are the Raman spectra of the char residuals of EP and EP/10%DABP–2DOPO, (c), (d) and (e) are the XPS spectra of char residuals.

resin could form a dense and stable phosphorus-rich char layer, reduce the passage of oxygen and flammable gases, and reduce the transfer of heat. Moreover, the mechanical properties of DOPO–2DABP had significantly improved. Given the coefficient of the biphenyl structure and DOPO group, the tensile strength and breaking elongation had improved simultaneously with the highest increases of 86.4% and 176.5%, respectively.

CRediT authorship contribution statement

Xueyan Dai: Visualization, Investigation, Conceptualization, Methodology, Writing - original draft. **Peihong Li:** Visualization, Investigation, Conceptualization, Methodology. **Yanlong Sui:** Conceptualization, Methodology. **Chunling Zhang:** Visualization, Investigation, Supervision.

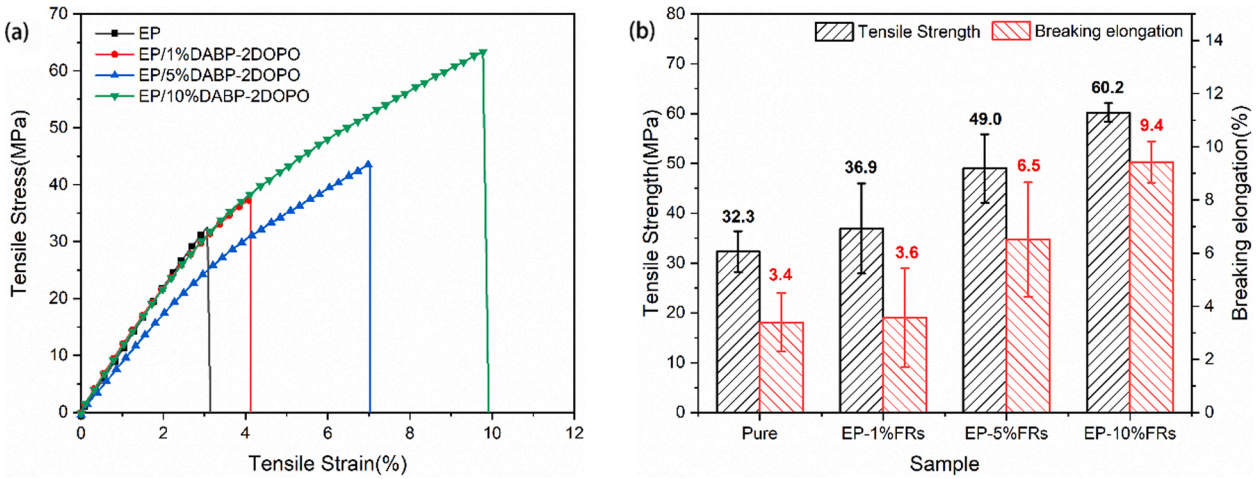

Fig. 11. Tensile properties of EP, EP/1%DABP–2DOPO, EP/5%DABP–2DOPO, and EP/10%DABP–2DOPO.

Declaration of Competing Interest

The authors declare that they have no known competing financial interests or personal relationships that could have appeared to influence the work reported in this paper.

Acknowledgment

The authors are grateful to the National Natural Science Foundation of China (No. 52073112), the Natural Science Foundation of Jilin Province (No. 20180101197jc), and the China International Science and Technology Cooperation Program (No. 20190701001GH).

Data Availability

The data used to support the findings of this study are available from the corresponding author upon request.

References

[1] J.C. Capricho, B. Fox, N. Hameed, Multifunctionality in Epoxy Resins, Polym. Rev. 60 (2020) 1–41, https://doi.org/10.1080/15583724.2019.1650063.
[2] P. Mohan, A Critical Review: The Modification, Properties, and Applications of Epoxy Resins, Polym. - Plast. Technol. Eng. 52 (2013) 107–125, https://doi.org/10.1080/03602559.2012.727057.
[3] F.L. Jin, X. Li, S.J. Park, Synthesis and application of epoxy resins: A review, J. Ind. Eng. Chem. 29 (2015) 1–11, https://doi.org/10.1016/j.jiec.2015.03.026.
[4] B. Perret, B. Schartel, K. Stöß, M. Ciesielski, J. Diederichs, M. Döring, J. Krämer, V. Altstädt, Novel DOPO-based flame retardants in high-performance carbon fibre epoxy composites for aviation, Eur. Polym. J. 47 (2011) 1081–1089, https://doi.org/10.1016/j.eurpolymj.2011.02.008.
[5] T. Cai, J. Wang, C. Zhang, M. Cao, S. Jiang, X. Wang, B. Wang, W. Hu, Y. Hu, Halogen and halogen-free flame retarded biologically-based polyamide with markedly suppressed smoke and toxic gases releases, Compos. Part B Eng. 184 (2020), 107737, https://doi.org/10.1016/j.compositesb.2019.107737.
[6] S. Liang, N.M. Neisius, S. Gaan, Recent developments in flame retardant polymeric coatings, Prog. Org. Coatings. 76 (2013) 1642–1665, https://doi.org/10.1016/j.porgcoat.2013.07.014.
[7] I. van der Veen, J. de Boer, Phosphorus flame retardants: Properties, production, environmental occurrence, toxicity and analysis, Chemosphere. 88 (2012) 1119–1153, https://doi.org/10.1016/j.chemosphere.2012.03.067.
[8] Q. Wang, W. Shi, Kinetics study of thermal decomposition of epoxy resins containing flame retardant components, Polym. Degrad. Stab. 91 (2006) 1747–1754, https://doi.org/10.1016/j.polymdegradstab.2005.11.018.
[9] X. Wang, Q. Chen, Y. Zheng, M. Hong, H. Fu, Study on novel flame retarded LDH-TDI-HEA-VTES-acrylate composites and their flame retardant mechanism, React. Funct. Polym. 147 (2020), 104371, https://doi.org/10.1016/j.reactfunctpolym.2019.104371.
[10] D.Y. Wang, A. Das, A. Leuteritz, R.N. Mahaling, D. Jehnichen, U. Wagenknecht, G. Heinrich, Structural characteristics and flammability of fire retarding EPDM/layered double hydroxide (LDH) nanocomposites, RSC Adv. 2 (2012) 3927–3933, https://doi.org/10.1039/c2ra20189e.
[11] Z. Yang, H. Peng, W. Wang, T. Liu, Optimum Compatibilization for the Nonflammability of Thermoplasticized Crosslinked Polyethylene/Metal Hydroxides Composites with a Compatibilizer, J. Appl. Polym. Sci. 116 (2010) 2658–2667, https://doi.org/10.1002/app.
[12] A. Yasemin, M. Doğan, E. Bayramlı, The effect of red phosphorus on the fire properties of intumescent pine wood flour – LDPE composites, FIRE Mater. (2009) 697–703, https://doi.org/10.1002/fam.
[13] U. Braun, B. Schartel, Flame retardant mechanisms of red phosphorus and magnesium hydroxide in high impact polystyrene, Macromol. Chem. Phys. 205 (2004) 2185–2196, https://doi.org/10.1002/macp.200400255.
[14] M. Pecht, Y. Deng, Electronic device encapsulation using red phosphorus flame retardants, Microelectron. Reliab. 46 (2006) 53–62, https://doi.org/10.1016/j.microrel.2005.09.001.
[15] F. Laoutid, L. Bonnaud, M. Alexandre, J.M. Lopez-Cuesta, P. Dubois, New prospects in flame retardant polymer materials: From fundamentals to nanocomposites, Mater. Sci. Eng. R Reports. 63 (2009) 100–125, https://doi.org/10.1016/j.mser.2008.09.002.
[16] T. Kawahara, A. Yuuki, K. Hashimoto, K. Fujiki, T. Yamauchi, N. Tsubokawa, Immobilization of flame-retardant onto silica nanoparticle surface and properties of epoxy resin filled with the flame-retardant-immobilized silica (2), React. Funct. Polym. 73 (2013) 613–618, https://doi.org/10.1016/j.reactfunctpolym.2013.01.001.
[17] D.A. Hypophosphite, Synergistic Flame-Retardant Mechanism of Dicyclohexenyl Aluminum Hypophosphite and Nano-Silica, Polymers (Basel). 1 (2019) 1211, https://doi.org/10.3390/polym11071211.
[18] Z. Fanglong, X. Qun, F. Qianqian, L. Rangtong, L. Kejing, Influence of nano-silica on flame resistance behavior of intumescent flame retardant cellulosic textiles: Remarkable synergistic effect? Surf. Coatings Technol. 294 (2016) 90–94, https://doi.org/10.1016/j.surfcoat.2016.03.059.
[19] L. Qu, Y. Sui, C. Zhang, P. Li, X. Dai, B. Xu, D. Fang, POSS-functionalized graphene oxide hybrids with improved dispersive and smoke-suppressive properties for epoxy flame-retardant application, Eur. Polym. J. 122 (2020), 109383, https://doi.org/10.1016/j.eurpolymj.2019.109383.
[20] B. Sang, Z. wei Li, X. hong Li, L. gui Yu, Z. jun Zhang, Graphene-based flame retardants: a review, J. Mater. Sci. 51 (2016) 8271–8295. https://doi.org/10.1007/s10853-016-0124-0.
[21] Y. Sui, L. Qu, P. Li, X. Dai, Q. Fang, C. Zhang, Y. Wang, Covalently functionalized graphene oxide wrapped by silicon-nitrogen-containing molecules: Preparation and simultaneous enhancement of the thermal stability, flame retardancy and mechanical properties of epoxy resin nanocomposites, RSC Adv. 10 (2020) 13949–13959, https://doi.org/10.1039/d0ra01866j.
[22] V.C.D. M. SPONTÓ N, J. C. RONDA, M. GALIA', Departament, Flame Retardant Epoxy Resins Based on Diglycidyl Ether of (2,5-Dihydroxyphenyl)diphenyl Phosphine Oxide M., J. Polym. Sci. Part A Polym. Chem. 45 (2007) 2142–2151. https://doi.org/10.1002/pola.
[23] N.M. Neisius, M. Lutz, D. Rentsch, P. Hemberger, S. Gaan, Synthesis of DOPO-based phosphonamidates and their thermal properties, Ind. Eng. Chem. Res. 53 (2014) 2889–2896, https://doi.org/10.1021/ie403677k.
[24] C.S. Wang, C.H. Lin, Novel phosphorus-containing epoxy resins. Part II: Curing kinetics, Polymer (Guildf). 41 (2000) 8579–8586, https://doi.org/10.1016/S0032-3861(00)00211-1.
[25] C.H. Lin, C.S. Wang, Novel phosphorus-containing epoxy resins Part I. Synthesis and properties, Polymer (Guildf). 42 (2001) 1869–1878, https://doi.org/10.1016/S0032-3861(00)00447-X.
[26] T.H. Ho, H.J. Hwang, J.Y. Shieh, M.C. Chung, Thermal and physical properties of flame-retardant epoxy resins containing 2-(6-oxido-6H-dibenz<c, e><1,2>oxaphosphorin-6-yl)-1,4-naphthalenediol and cured with dicyanate ester, Polym. Degrad. Stab. 93 (2008) 2077–2083, https://doi.org/10.1016/j.polymdegradstab.2008.09.002.
[27] Y. Zhang, G. Xu, Y. Liang, J. Yang, J. Hu, Preparation of flame retarded epoxy resins containing DOPO group, Thermochim. Acta. 643 (2016) 33–40, https://doi.org/10.1016/j.tca.2016.09.015.

[28] K.A. Salmeia, S. Gaan, An overview of some recent advances in DOPO-derivatives: Chemistry and flame retardant applications, Polym. Degrad. Stab. 113 (2015) 119–134, https://doi.org/10.1016/j.polymdegradstab.2014.12.014.
[29] S. Brehme, T. Köppl, B. Schartel, O. Fischer, V. Altstädt, D. Pospiech, M. Döring, Phosphorus polyester - An alternative to low-molecular-weight flame retardants in poly(butylene terephthalate)? Macromol. Chem. Phys. 213 (2012) 2386–2397, https://doi.org/10.1002/macp.201200072.
[30] W. Zhang, X. Li, X. Guo, R. Yang, Mechanical and thermal properties and flame retardancy of phosphorus-containing polyhedral oligomeric silsesquioxane (DOPO-POSS)/ polycarbonate composites, Polym. Degrad. Stab. 95 (2010) 2541–2546, https://doi.org/10.1016/j.polymdegradstab.2010.07.036.
[31] T. Yu, T. Tuerhongjiang, C. Sheng, Y. Li, Phosphorus-containing diacid and its application in jute/poly(lactic acid) composites: Mechanical, thermal and flammability properties, Compos. Part A Appl. Sci. Manuf. 97 (2017) 60–66, https://doi.org/10.1016/j.compositesa.2017.03.004.
[32] M. Niu, Z. Zhang, Z. Wei, W. Wang, Effect of a novel flame retardant on the mechanical, thermal and combustion properties of poly(Lactic acid), Polymers (Basel). 12 (2020) 1–15, https://doi.org/10.3390/polym12102407.
[33] C.S. Wang, C.H. Lin, Synthesis and Properties of Phosphorus-Containing Epoxy Resins by Novel Method, J. Polym. Sci. Part A Polym. Chem. 37 (1999) 3903–3909.
[34] H.E. Kissinger, Reaction Kinetics in Differential Thermal Analysis, Anal. Chem. 303 (1957) 1702–1706, https://doi.org/10.1021/ac60131a045.
[35] T. Ozawa, Kinetics of non-isothermal crystallization, Polymer (Guildf). 12 (1971) 150–158.
[36] Y.L. Liu, Flame-retardant epoxy resins from novel phosphorus-containing novolac, Polymer (Guildf). 42 (2001) 3445–3454, https://doi.org/10.1016/S0032-3861(00)00717-5.
[37] C.S. Wang, J.Y. Shieh, Phosphorus-containing epoxy resin for an electronic application, J. Appl. Polym. Sci. 73 (1999) 353–361, https://doi.org/10.1002/(SICI)1097-4628(19990718)73:3<353::AID-APP6>3.0.CO;2-V.
[38] L. Qu, C. Zhang, P. Li, X. Dai, T. Xu, Y. Sui, J. Gu, Y. Dou, Improved thermal properties of epoxy resin modified with polymethyl methacrylate-microencapsulated phosphorus-nitrogen-containing flame retardant, RSC Adv. 8 (2018) 29816–29829, https://doi.org/10.1039/c8ra05911j.
[39] L. Wang, J. Jiang, P. Jiang, Synthesis characteristic of a novel flame retardant containing phosphorus silicon and its application in ethylene vinyl-acetate copolymer (EVM) rubber, J. Polym. Res. 17 (2010) 891–902, https://doi.org/10.1007/s10965-009-9381-9.
[40] L. Gao, D. Wang, Y. Wang, J. Wang, B. Yang, A flame-retardant epoxy resin based on a reactive phosphorus-containing monomer of DODPP and its thermal and flame-retardant properties, Polym. Degrad. Stab. J. 93 (2008) 1308–1315, https://doi.org/10.1016/j.polymdegradstab.2008.04.004.
[41] W. Cai, Y. Hu, Y. Pan, X. Zhou, F. Chu, L. Han, X. Mu, Z. Zhuang, X. Wang, W. Xing, Self-assembly followed by radical polymerization of ionic liquid for interfacial engineering of black phosphorus nanosheets: Enhancing flame retardancy, toxic gas suppression and mechanical performance of polyurethane, J. Colloid Interface Sci. 561 (2020) 32–45, https://doi.org/10.1016/j.jcis.2019.11.114.